DRAFT

CONF-770321--7

NEUTRON YIELDS AND DOSIMETRY FOR Be(d,n) AND Li(d,n) NEUTRON SOURCES AT E_d = 40 MeV*

M. J. Saltmarsh, C. A. Lundmann, C. B. Fulmer, and R. C. Stylest
Oak Ridge National Laboratory
Oak Ridge, Tennessee 37830

Time-of-flight measurements are reported for the thick-target neutron yields from the Be(d,n) and Li(d,n) reactions over an angular range of 0–90° at a deuteron energy of 40 MeV. Foil activation mreasurements are also described for the Be(d,n) reaction. A dosimetry technique based on these measurements is discussed. [Dosimetry: measured thick-target neutron yields, Be(d,n), Li(d,n); E_d = 40 MeV; E_n > 2 MeV; θ = 0–90°.]

Introduction

In recent years there has been growing interest in the use of neutron sources based on the Be(d,n) and Li(d,n) reactions for fusion-related materials studies. In this paper we report on measurements of the thick-target neutron yields from these two reactions which were made using a 40-MeV deuteron beam from the Oak Ridge Isochronous Cyclotron (ORIC). Time-of-flight (TOF) data were obtained for both reactions over the angular range 0 to 90°, and foil activation measurements were made for the Be(d,n) reaction in the range 0 to 90°. The results were used to develop a dosimetry technique suitable for the existing ORIC Be(d,n) neutron source,[1] and to evaluate the performance expected from the recently proposed Li(d,n) intense neutron sources.[2]

---

*Research sponsored by Energy Research and Development Administration under contract with Union Carbide Corporation.

†Oak Ridge Associated University undergraduate trainee. Present address: University of Georgia, Athens, Georgia.

Time-of-Flight Measurements

The time-of-flight (TOF) measurements were made using a 40.0-MeV deuteron beam from the ORIC. This beam is pulsed at the cyclotron orbital frequency of 12.97 MHz, providing 2-ns-wide pulses every 77.01 ns. With the maximum available flight-path of 3 m the resultant energy resolution varied from ~4% at a neutron energy of 5 MeV to ~15% at 40 MeV. However, neutron energies below 5 MeV could not be reliably measured with this flight path because of overlapping events from successive beam bursts. Accordingly most of the measurements were repeated using a flight path of 0.75 m, which allowed the data to be extended down to $E_n \sim 2$ MeV.

The experimental arrangement is shown in Fig. 1. The deuteron beam passed through a thin (7.5 mg/cm^2) gold scattering foil, used in monitoring the beam, and onto the thick beryllium (or lithium) target. Neutrons and gamma rays emitted at an angle θ were detected in a cylindrical cell of NE213 liquid scintillator* 37.3 mm in diameter by 34.1 mm long viewed by a 56AVP photomultiplier tube. The fast timing signal from the photomultiplier tube was used to start a time-to-amplitude converter, the stop signal being derived from every second cycle of the cyclotron RF. A neutron-gamma discrimination circuit was used to route an event into one of two 400-channel TOF spectra. Background events, for example neutrons scattered from the experimental room floor or walls, were measured by placing a 20-cm-thick lead shadow shield midway between the target and the detector. When the lead shield was removed, it was displaced by the smallest possible distance (6 cm), so that the effect of in-scattering from the lead was similar for both foreground and background runs.

*Manfactured by Nuclear Enterprises, Inc., 935 Terminal Waym San Carlos, CA 94070.

The beam current required for these measurements was small, ≤ 0.1 nA. The beam was monitored by counting deuterons scattered at $\pm 45°$ from the thin gold foil. Two detectors were used to eliminate errors due to movements of the beam spot on the gold foil. This secondary monitor was calibrated at intervals during the experiment by increasing the beam current and using the second scattering chamber as a Faraday Cup.

The neutron detector threshold was set relative to the half-height of the Compton edge from a ^{22}Na source. Following the definitions of Verbinski et al.[3] this corresponds to 0.89 light units (LU). For the 3-m runs the threshold was set to be 1.00 LU ($E_n \sim 3.5$ MeV), while for the 0.75-m data a setting of 0.266 LU ($E_n \sim 1.3$ MeV) was used. The detector efficiency at each threshold was calculated for a number of neutron energies in the range 1–50 MeV, using the Monte Carlo code 05S.[4]

For data analysis the positions of the two gamma peaks in the appropriate spectrum were obtained by fitting a gaussian peak to the data. The time calibration was obtained from these peak locations by assuming a linear dependence of TOF versus channel number. The neutron spectrum was then converted to an energy spectrum, defining the flight path to be the distance from the geometrical center of the target to the geometrical center of the liquid scintillator. Allowance was made for neutron absorption in the aluminum walls of the scattering chamber (~3 mm thick) and the scintillator cell (~1.5 mm thick) as well as the air along the flight path. The measured energy spectra from d + Be at 0 and 90° are shown in Fig. 2, with the error bars showing statistical uncertainties only. The data from d + Be and d + Li at all angles studied are shown as smooth curves in Figs. 3 and 4, respectively. The curves for 7 and 45° do not extend below 5 MeV as no runs were made at these angles with a 0.75-m flight path.

Monitor uncertainties for the 0.75-m data were typically 8–15% as against 3–4% for the 3-m data. Accordingly, the relative normalization for the two data sets was derived from the total neutron yields for 7.5 MeV < E_n < 12.5 MeV, and the overall normalization defined by the monitor counts for the 3-m data.

The experimental uncertainties for these data come from three sources. First, there are the statistical uncertainties indicated by the error bars in Fig. 2. These are generally small. Second, there is a beam monitor uncertainty at each angle, which amounts to approximately 4% at all angles, except for 45° where it is 6%. Finally, and most important, there are uncertainties due to the errors in the efficiency calculations. The resultant overall normalization uncertainty is estimated to be ±15%. Errors in the measured shape of the energy spectrum due to errors in the shape of the efficiency curve are difficult to assess, but are probably less than 10%.

Foil Activation Measurements

The activation measurements of the Be(d,n) neutron yields required much higher deuteron beam intensities than did the TOF measurements. Therefore, the existing ORIC neutron source, which comprises a water-cooled beryllium target, was used; permitting deuteron beam intensities = 20 μA. In order to make these measurements in a well-defined geometry the activation foils were placed at a distance from the target which was large compared to the dimensions of the interaction region within the beryllium target. The arrangement adopted is shown schematically in Fig. 5. Rectangular foils, 50 x 120 mm, were mounted on a support in the shape of a circular arc 76.2 mm in radius, and the whole assembly located with the center of the arc at the center of the d + Be interaction region. After exposure for 4 hr at a deuteron

beam level of 20 μA, the foils were removed, allowed to cool for several days, and 6.3-mm-diam discs were punched from them in the pattern indicated in Fig. 5. The discs were weighed and the gamma activities listed in Table 1 were measured using a Ge(Li) detector whose efficiency was calibrated using a standard source.

Table 1. Reactions Used for Activation Measurements

Reaction	Q-Value (MeV)	E_γ (keV)
$^{58}Ni(n,p)^{58}Co$	0.39	810.5
$^{59}Co(n,2n)^{58}Co$	−10.47	810.5
$^{93}Nb(n,2n)^{92m}Nb$	−8.95	934

To convert the measured activities to neutron yields the spectrum-averaged cross sections for the three reactions were computed as a function of scattering angle by folding the spectrum shapes as measured in the TOF runs with the excitation functions shown in Fig. 6. For energies ≤20 MeV the available data[5,6] for the $^{59}Co(n,2n)$ and $^{93}Nb(n,2n)$ reactions appear to be in reasonably good agreement, but considerable scatter of the experimental results is apparent for the $^{58}Ni(n,p)$ case.[7] Above 20 MeV there are no data, so the excitation functions were extrapolated using the shapes calculated with the code THRESH.[8] The overall uncertainties in the calculated spectrum averaged cross sections were estimated to be ±10% for the $^{59}Co(n,2n)$ and $^{93}Nb(n,2n)$ reactions, and ±15% for the $^{58}Ni(n,p)$ reaction. In Fig. 7 we show the experimental values of neutron yield (E_n > 2 MeV)

versus angle obtained from the three activation foils, corrected for absorption in the tantalum end plate. The TOF data are also shown. The error bars indicate statistical uncertainties only. The solid line represents the mean of the TOF and activation results. The four sets of data are displaced from this curve by an average of −10% (TOF), +10%, [^{59}Co(n,2n)], +1% [^{93}Nb(n,2n)], and −15% [^{58}Ni(n,p)], in reasonable agreement with the estimated uncertainties.

In Table 2 the results of four separate measurements of d + Be neutron yields (E_n > 2 MeV) are listed, together with the average values represented by the solid line in Fig. 7.

The total d + Li neutron yields for E_n > 2 MeV are given in Table 3. From the beryllium data we see that the TOF results are 10% lower than the average values for the total yields, accordingly the lithium data should be renormalized upwards by this amount, as shown in the final column of Table 3. The errors quoted in this column reflect not only statistical errors, but also those due to uncertainties in the shape of the detector efficiency curves.

Thick-target neutron yields from the d + Be reaction have previously been measured by Schweimer[9] at E_d = 40 and 53.8 MeV, and by Meulders et al.[10] at E_d = 16, 33, and 50 MeV. Schweimer's measurement of the neutron energy spectrum at 0° extends down to a neutron energy of 11.5 MeV, and the shape is in good agreement with out results, however, his estimate of the overall yield is approximately 35% lower. Meulders' data include energy spectra at a number of angles for neutron energies E_n > 3 MeV. No direct comparison with these data is possible due to the differing deuteron energies, but our data follow the same trends as regards spectral shapes, angular distributions and overall yields.

Table 2. Thick-Target Neutron Yields ($E_n > 2$ MeV) from d + Be, E_d = 40 MeV
Units are 10^{10} n/μC/sr

Scattering Angle (deg)	Neutron Yields				Average[a]
	TOF Data	Activation Data			
		^{59}Co(n,2n)	^{58}Ni(n,p)	^{93}Nb(2,2n)	
0	33.6 ± 1.3	38.7 ± 0.4	30.9 ± 0.3	35.7 ± 0.4	36.0 ± 1.8
5		33.7 ± 0.4	24.8 ± 0.3	29.9 ± 0.3	30.0 ± 1.5
7	25.1 ± 1.3				26.6 ± 1.3
10		26.0 ± 0.2	18.0 ± 0.2	23.1 ± 0.2	22.2 ± 1.1
15	13.2 ± 0.5	18.5 ± 0.3			15.4 ± 0.8
20		13.4 ± 0.2	9.51 ± 0.13	11.6 ± 0.2	11.7 ± 0.6
30	6.8 ± 0.2	9.26 ± 0.17	6.59 ± 0.11	8.19 ± 0.2	8.1 ± 0.4
40		7.29 ± 0.23	5.12 ± 0.12	6.65 ± 0.2	5.9 ± 0.3
45	4.2 ± 0.25				5.05 ± 0.25
50		4.86 ± 0.15	3.74 ± 0.06	4.36 ± 0.16	4.30 ± 0.22
60	2.77 ± 0.1	3.30 ± 0.13	2.79 ± 0.07	3.34 ± 0.11	3.14 ± 0.16
70		2.21 ± 0.16	2.10 ± 0.08	2.31 ± 0.14	2.30 ± 0.12
80		1.66 ± 0.16	1.68 ± 0.06	1.39 ± 0.08	1.67 ± 0.08
90	1.26 ± 0.04				1.21 ± 0.06
Scale uncertainty	±15%	±10%	±15%	±10%	±7%

[a]Corresponds to solid line in Fig. 7.

Table 3. Thick Target Neutron Yields (E_n > 2 MeV) from d + Li, E_d = 40 MeV

Units are 10^{10} n/μC/sr

Scattering Angle (deg)	Neutron Yield	
	TOF Data[a]	Renormalized
0	36.7 ± 1.8	40.9 ± 2.9
7	25.3 ± 1.3	38.2 ± 2.0
15	11.6 ± 0.4	13.0 ± 0.9
30	6.28 ± 0.25	6.99 ± 0.50
45	3.73 ± 0:17	4.15 ± 0.30
60	2.48 ± 0.09	2.76 ± 0.19
90	1.43 ± 0.05	1.59 ± 0.11
Scale uncertainty	±15%	±7%

[a]Statistical errors only.

Dosimetry for the d + Be Neutron Source

All the yield measurements described in the previous section were made in well-defined geometries. However, irradiations performed with the ORIC source generally require samples to be placed within a few millimeters of the beryllium target so that a given position on the sample corresponds to a range of scattering angles from the target. Furthermore both the neutron flux and the energy spectrum vary strongly with distance from the beam axis. Thus the dosimetry must provide a measure of both quantities with a spatial resolution ~1 mm. The basis of the method is to assume that the neutron energy spectrum at any point on the sample is adequately represented by the neutron spectrum seen far from the target at some effective scattering angle (θ_{eff}). Then the neutron dose at a given point on the sample can be completely described by two numbers, the total neutron yield for $E_n > 2$ MeV and the spectrum shape parameter θ_{eff}.

The response of the nickel and cobalt foils in terms of these two parameters is obtained from the yield measurements described in the preceding section. From the activation measurements done in a well-defined geometry, the ratio of the cobalt and nickel activities at each scattering angle are obtained, and used to calculate the ratio of the spectrum averaged cross sections, $\bar{\sigma}(Co)/\bar{\sigma}(Ni)$, as a function of angle. The results are shown in Fig. 8. The solid line in Fig. 7, which is our best estimate of the total neutron yield, is used in conjunction with the same activation measurements to calculate the values of $\bar{\sigma}(Co)$ and $\bar{\sigma}(Ni)$ as function of scattering angle. These results (a) are given in Table 4, together with the values (b) previously estimated from the TOF data and the published cross sections.

Table 4. Estimates of the Spectrum-Averaged Cross Sections (in mb) for Various Reactions as a Function of Scattering Angle. Values labeled (a) are used for dosimetry (see text). Values labeled (b) were calculated from TOF data and available cross-section data.

Scattering Angle (deg)	$^{58}Ni(n,p)^{58}Co$		$^{59}Co(n,2n)^{58}Co$		$^{93}Nb(n,2n)^{92m}Nb$	
	$\bar{\sigma}$(Ni)		$\bar{\sigma}$(Co)		$\bar{\sigma}$(Nb)	
	(a)*	(b)	(a)	(b)	(a)	(b)
0	270	316 ± 47	424	394 ± 39	205	210 ± 20
5	270		400		195	
7	270	330 ± 50	383	332 ± 33	187	183 ± 18
10	272		348		174	
15	278	341 ± 51	300	257 ± 26	149	146 ± 15
20	283		260		131	
30	298	369 ± 55	212	186 ± 19	116	117 ± 12
40	313		175		103	
45	320	386 ± 58	161	168 ± 17	98	113 ± 11
50	329		148		93	
60	343	375 ± 56	124	116 ± 12	83	83 ± 8
70	361		101		74	
80	380		87		67	
90	400	368 ± 55	72	76 ± 8	58	60 ± 6

*Includes contributions from competing reactions such as $^{60}Ni(n,t)^{58}Co$.

[Strictly speaking the nickel values include a contribution from competing reactions such as $^{60}Ni(n,t)^{58}Co$, however, the correction is probably <5% and does not affect the present discussion.] The dosimetry procedure which we use is to measure the activity induced on cobalt and nickel foils at a given location, compute the ratio $\bar{\sigma}(Co)/\bar{\sigma}(Ni)$ and then obtain θ_{eff} from Fig. 8. Knowing θ_{eff} the value of $\bar{\sigma}(Co)$ [or $\bar{\sigma}(Ni)$] can be obtained from Table 4. and the total neutron fluence calculated.

An example of the method is illustrated in Fig. 9. The cobalt and nickel foils were in the form of 25-mm-diam discs, approximately 0.05 mm thick, placed perpendicular to the beam axis at a distance of 10 mm from the center of the beryllim target. After an irradiation lasting ~26 hr, the pair of foils was removed and allowed to cool for several weeks. Discs 1.5 mm in diameter were then punched from the foils in the radial pattern shown on the insert of the upper part of Fig. 9. Each small disc was weighed, and the 810-keV γ-activity measured with a Ge(Li) detector. From these data the location of the center of the neutron spot (i.e., the maximum activity) was estimated, and the activity of each disc plotted against its distance r from this center, as shown in Fig. 9. There is an implicit assumption in this procedure that the neutron intensity contours are circular, which appears to be well justified by the small scatter of the data points in these plots. From the data in the upper part of Fig. 9 the two dose parameters, θ_{eff} and neutron yield were calculated and plotted as a function of r as shown in the lower part of the figure. The neutron spot is seen to have a roughly gaussian profile, with a full width at half maximum of 8.5 mm, and a maximum of $\sim 2 \times 10^{17}$ n/cm^2, corresponding to an average flux $\sim 2.1 \times 10^{12}$ n/cm^2/sec during the irradiation.

The overall uncertainty in the neutron fluence is estimated to be ±10% due largely to the 7% uncertainty of the yield measurements used to calibrate the activation foils. The uncertainty in the definition of spectral shape is difficult to quantify, but in terms of the effective scattering angle it amounts to ±2°, as indicated in Fig. 9.

Summary

The neutron yield data described above provide an adequate basis for assessing the performance of Be(d,n) and Li(d,n) neutron sources which use a 40-MeV deuteron beam. It would be useful to extend these measurements to lower neutron energies ($E_n < 2$ MeV), although the contribution of such neutrons to the total radiation damage is not large (≤10%), at least in the high-flux regions of the neutron sources.

Because of the similarity of the spectral shapes from the Be(d,n) and Li(d,n) reactions, the dosimetry technique developed for the ORIC Be(d,n) source should be also applicable to Li(d,n) sources. However, more accurately known neutron activation cross sections are needed, particularly in the energy region $E_n > 15$ MeV. There will also be a need for measurements of transmutation product cross sections, particularly those for hydrogen and helium. Integral measurements for helium production could be made with existing Be(d,n) sources and would provide a useful check on the theoretical predictions.

References

1. M. J. Saltmarsh, C. A. Lundemann, C. B. Fulmer, and R. C. Styles, "Characteristics of an Intense Neutron Source Based on the d + Be Reaction," (submitted to Nucl. Inst. and Meth.).
2. M. J. Saltmarsh and R. E. Worsham (ED.), ORNL-TM-5223 (1976).
3. V. V. Verbinski, W. R. Burrus, T. A. Love, W. Zobel, N. W. Hill, and R. Textor, Nucl. Inst. and Meth. 65, 8 (1968).
4. R. E. Textor and V. V. Verbinski, ORNL-4160 (1968).
5. ENDF-B-IV, MAT-1199, BNL 17541 (ENDF-201) (1975).
6. A. Paulsen and R. Widera, Z. Physik 238, 23 (1970).
7. ENDF-B-IV, MAT-1190, BNL 17541 (ENDF-201) (1975).
8. S. Pearlstein, J. Nucl. Eng. 27, 81 (1973).
9. G. W. Schweimer, Nucl. Phys. A100, 537 (1967).
10. J. P. Moulders, P. Leleux, P. C. Marq, and C. Pirart, Phys. Med. Biol. 20, 235 (1975).

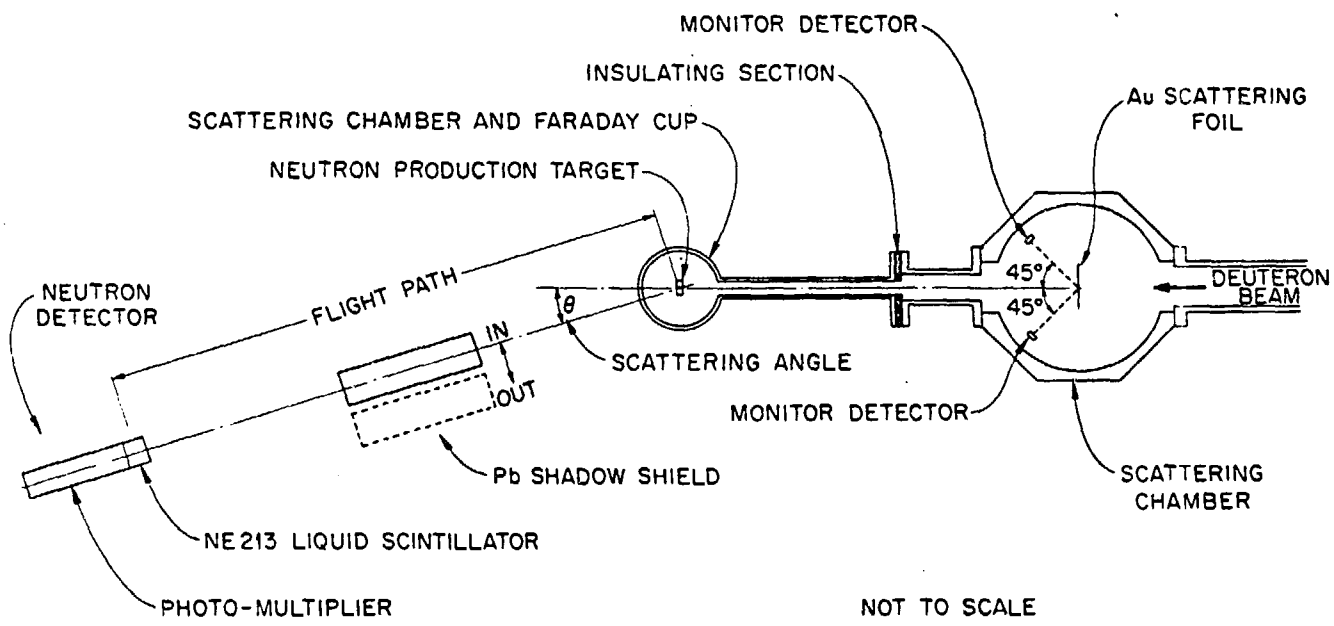

Fig. 6.1. The lay-out of the time-of-flight apparatus.

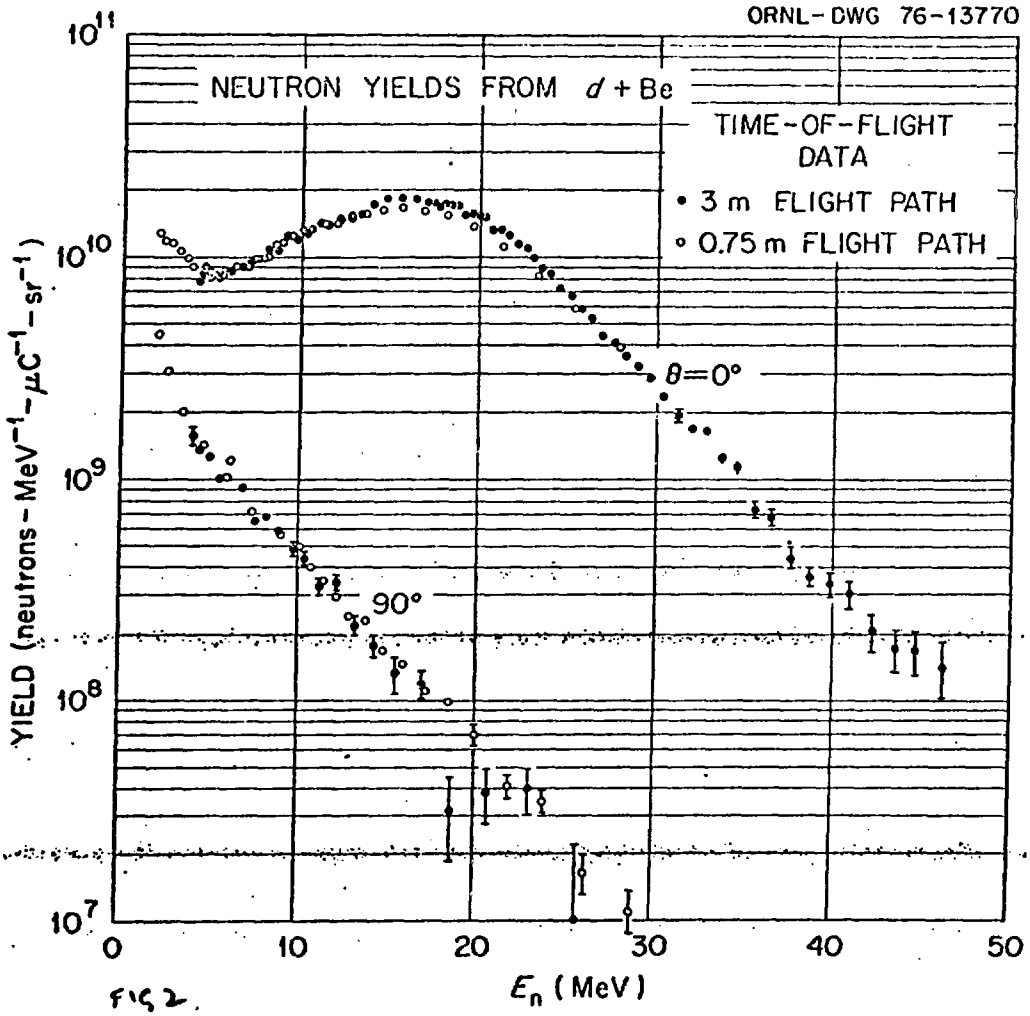

~~Fig. 4.~~ Time-of-flight data from 40 MeV deuterons on a thick Be target, showing representative error bars. The 0.75 m data (open circles) have been normalized to the 3 m data in the energy ranges 7.5 MeV < E_n < 12.5 MeV. The system resolution (3m data) varies from $\approx$ 200 keV at E_n = 5 MeV to $\approx$ 6 MeV at E_n = 40 MeV.

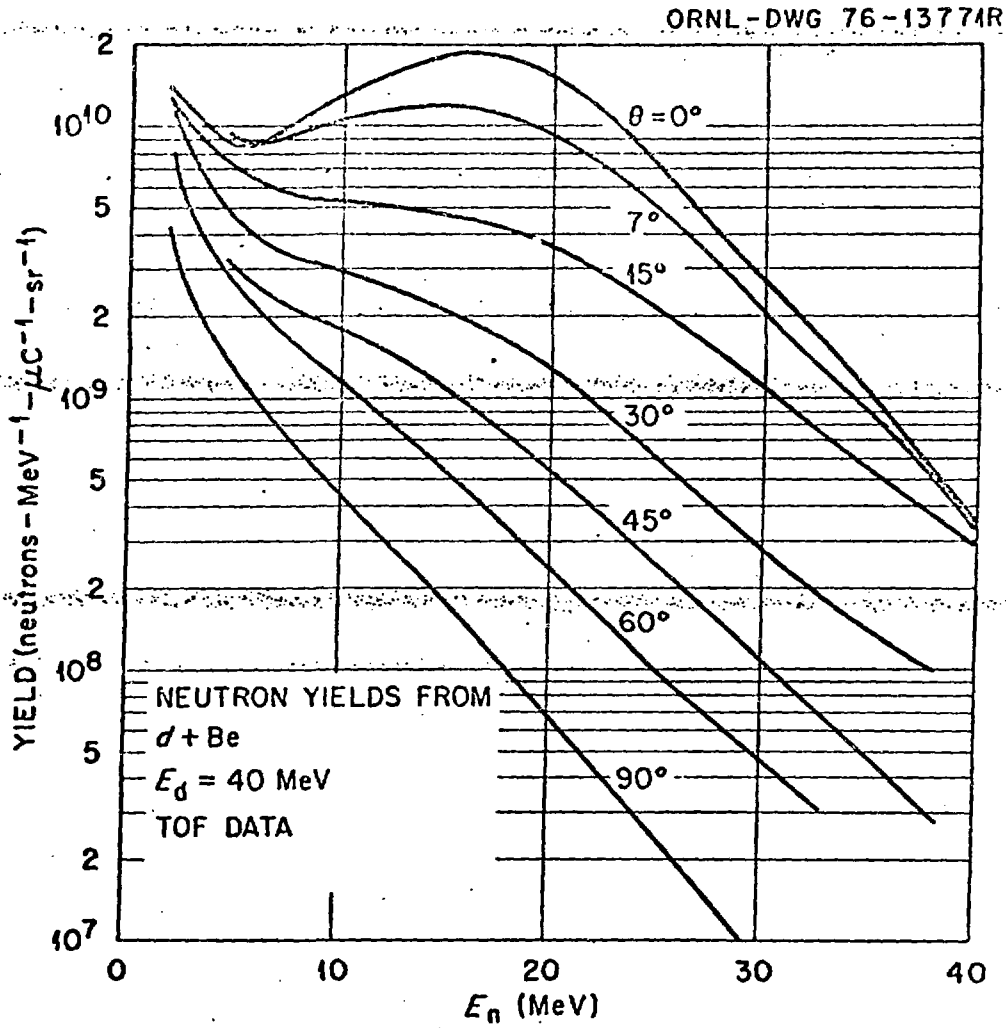

Fig. 3. Time-of-flight data obtained by drawing smooth curves through the results typified by those in Fig. 2.

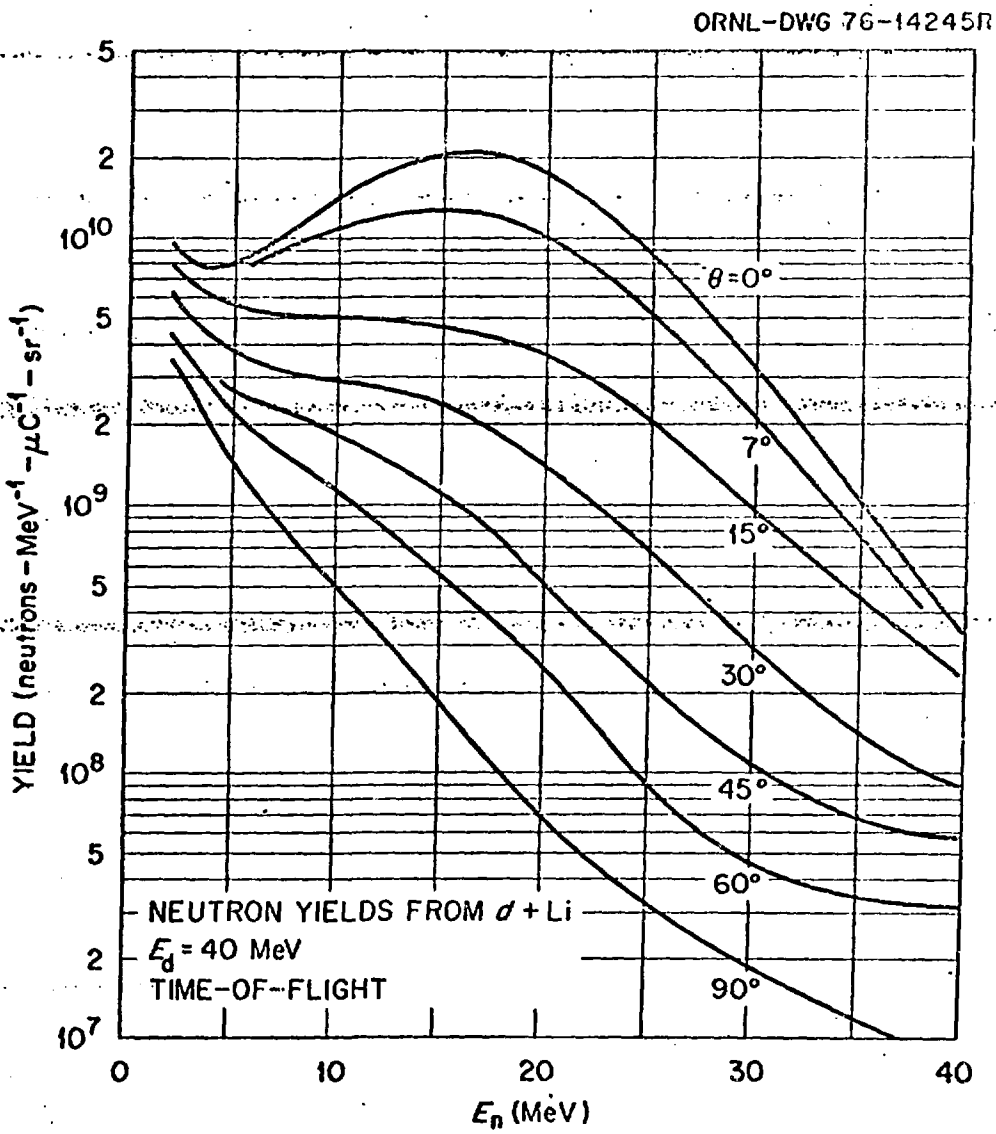

Fig. 4. Neutron yields from 40 MeV deuterons on a thick Li target. The curves were obtained from time-of-flight data in the same manner as those for d + Be (fig. 5).

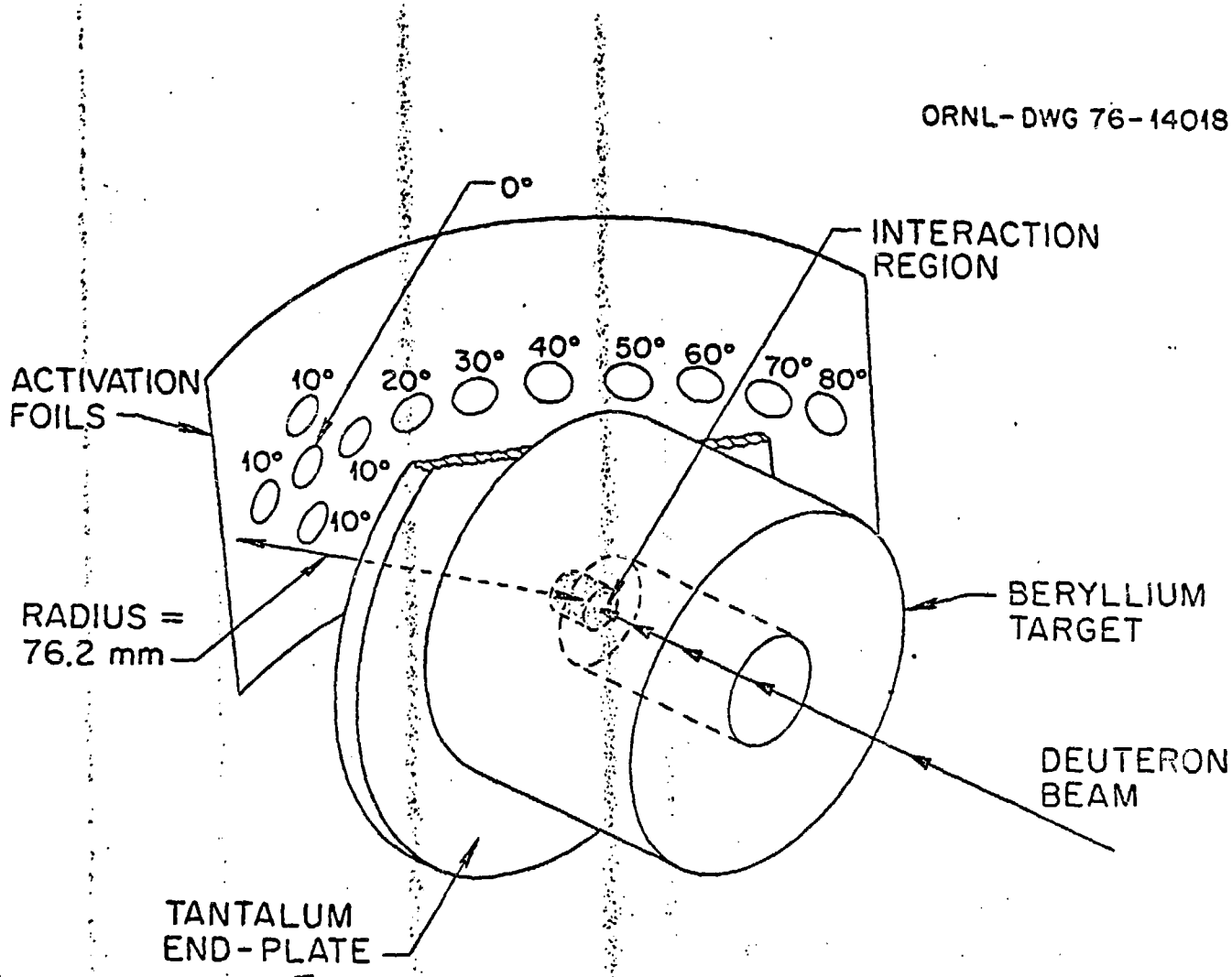

Fig. 5. The experimental arrangement used for the activation measurements in a well-defined geometry. The dimensions of the interaction region were length 6mm, diameter < 5 mm.

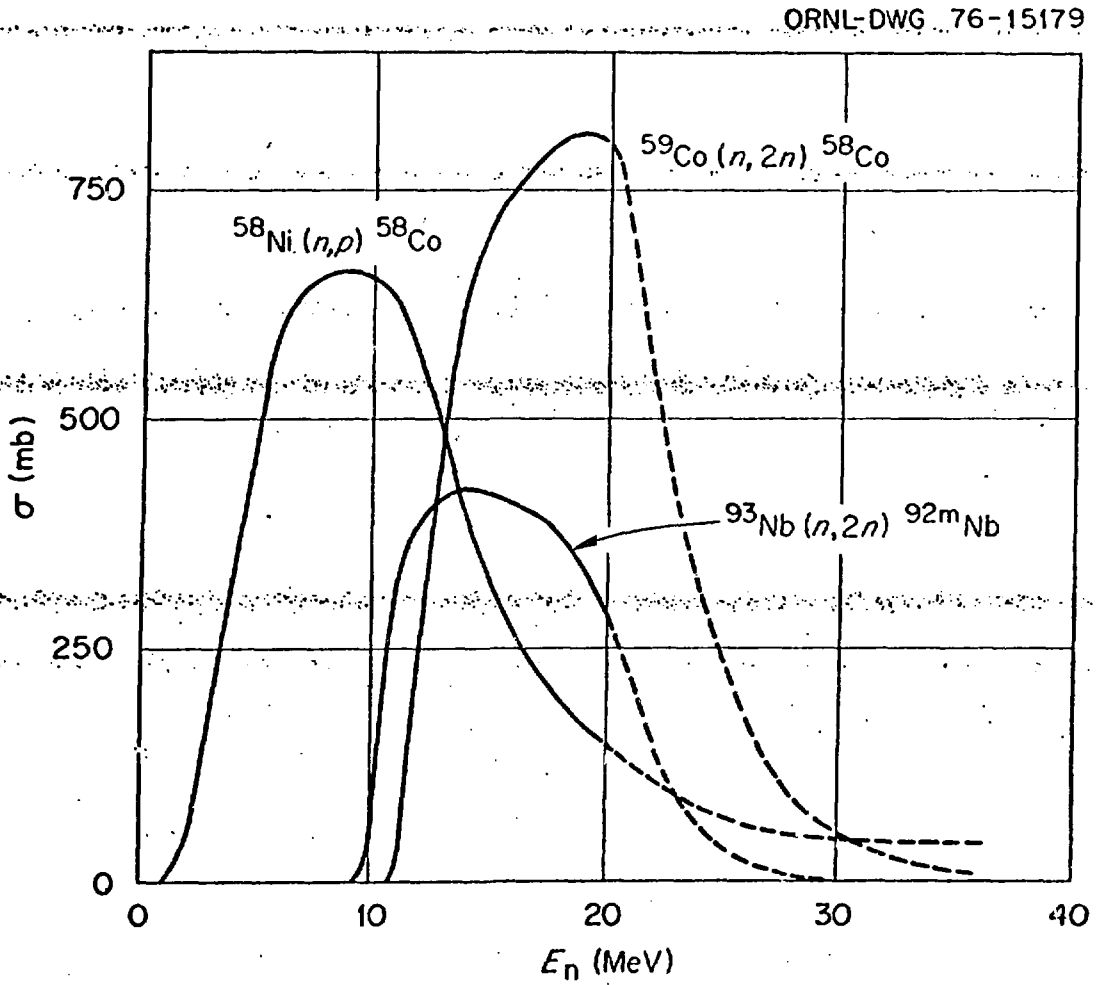

Fig. 6. Excitation functions used to calculate spectrum averaged cross sections. The solid lines represent the energy regions for which data (5, 6, 7) were available ; the dotted portions were extrapolations derived from Ref. 8.

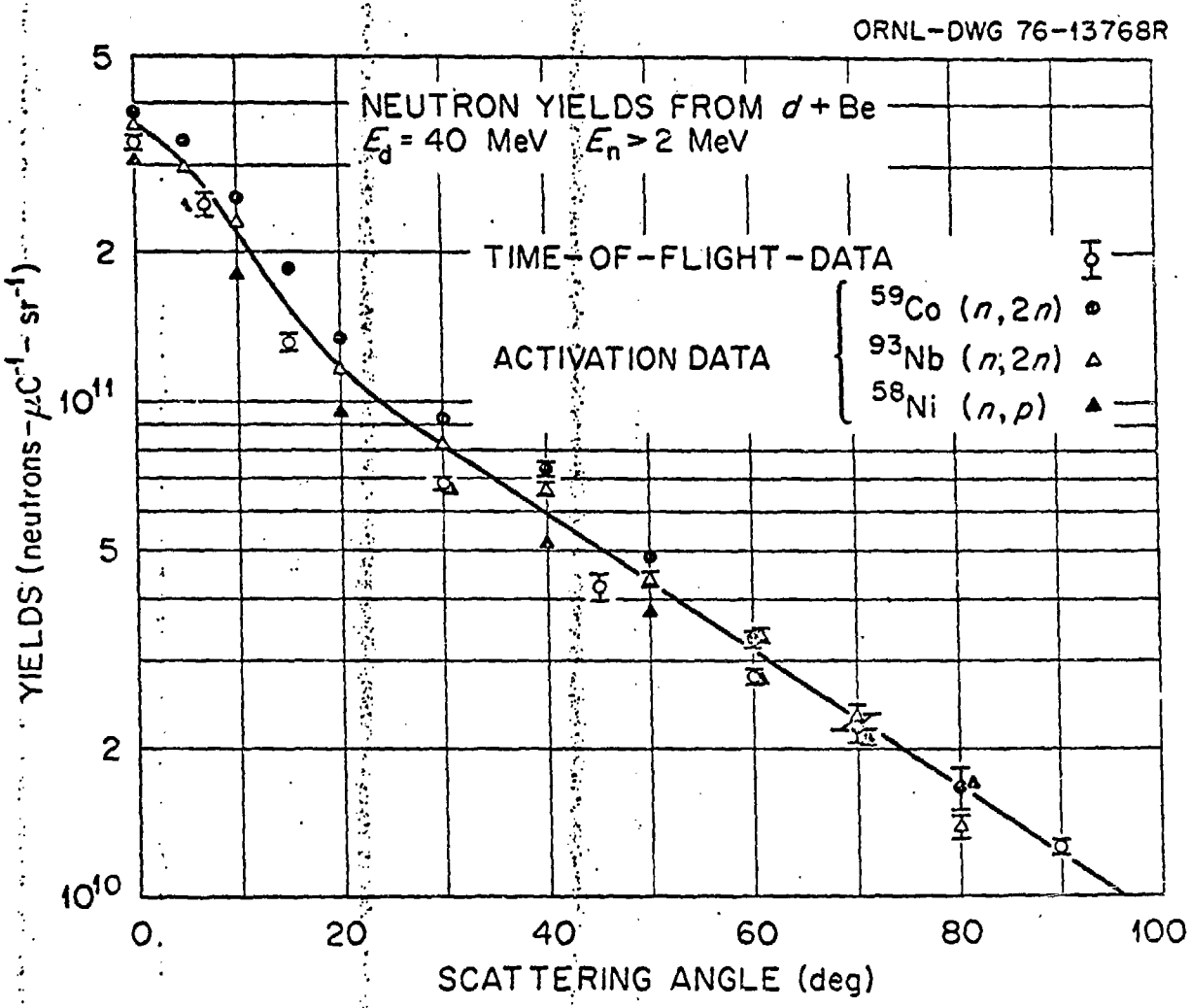

Fig. 7. Experimental values of neutron yield obtained in the present work for 40 MeV deuterons on thick beryllium targets.

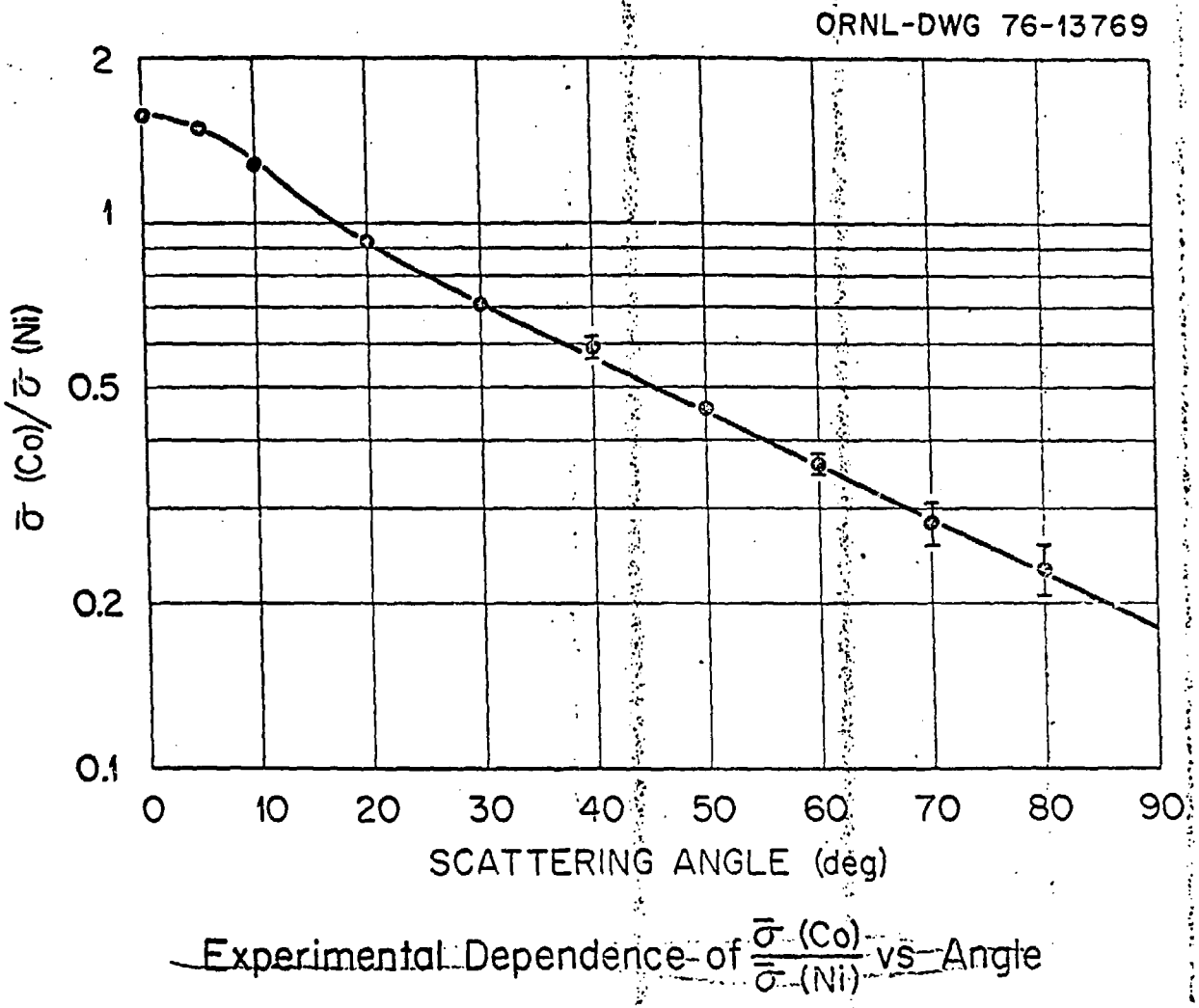

Fig. 6. Experimental dependence of $\bar{\sigma}(Co)/\bar{\sigma}(Ni)$ as a function of angle for neutrons emitted from a thick target bombarded with 40 MeV deuterons.

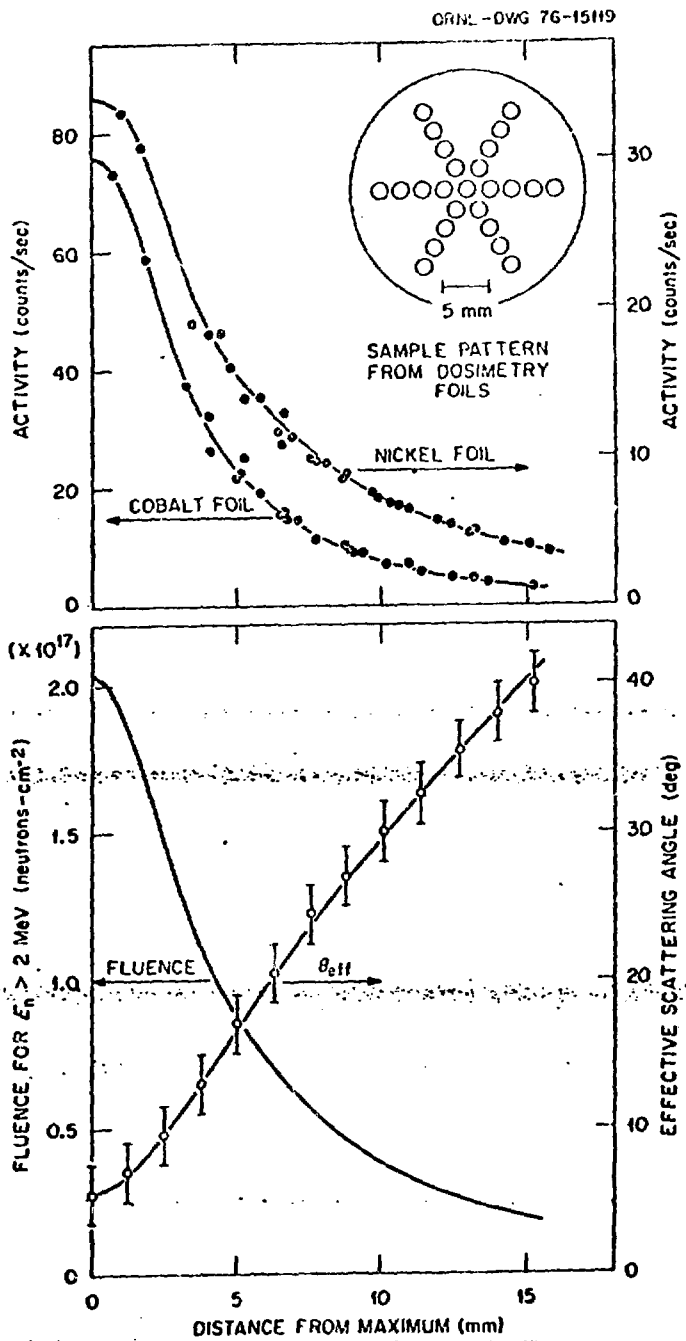

Fig. 9. Dosimetry method used for d + Be neutron source. The upper graphs show the distribution of ^{58}Co activity for the cobalt and nickel dosimetry foils. The lower plots show the spatial dependence of θ_{eff} and neutron yield inferred from these measurements ~~(see section 4)~~.